Available online at www.sciencedirect.com
ScienceDirect
Acta Biomaterialia 3 (2007) 944–951
Acta BIOMATERIALIA
www.elsevier.com/locate/actabiomat

Tribological behavior of plasma-sprayed carbon nanotube-reinforced hydroxyapatite coating in physiological solution

Kantesh Balani [a], Yao Chen [a], Sandip P. Harimkar [b], Narendra B. Dahotre [b], Arvind Agarwal [a,*]

[a] Department of Mechanical and Materials Engineering, Florida International University, Miami, FL 33174, USA
[b] Department of Materials Science and Engineering, University of Tennessee, Knoxville, TN 37996, USA

Received 3 March 2007; received in revised form 1 June 2007; accepted 4 June 2007
Available online 16 June 2007

Abstract

Wear behavior of plasma-sprayed carbon nanotube (CNT)-reinforced hydroxyapatite (HA) coating is evaluated in the simulated body fluid environment. Apart from enhancing the fracture toughness and providing biocompatibility, CNT-reinforced HA coating demonstrated superior wear resistance compared with that of hydroxyapatite coating without CNT. Initiation and propagation of microcracks during abrasive wear of plasma-sprayed hydroxyapatite coatings was suppressed by CNT reinforcement. Surface characterization and wear studies have shown that in addition to acting as underprop lubricant, CNTs provide reinforcement via stretching and splat-bridging for enhanced abrasion resistance in vitro.

Keywords: Hydroxyapatite; Carbon nanotubes; Plasma spraying; Wear; Simulated body fluid

1. Introduction

Replacing bone substances lost due to traumatic or non-traumatic events has been of particular interest in the development of orthopedic applications, leading to an ever-increasing need for fabrication of artificial hard tissue replacement implants. Among these hard tissue replacement materials, metallic implants have been widely used for orthopedic implants. However, there are concerns regarding the occurrence of corrosion, wear and negative tissue reaction, which always prevent proper distribution of stresses and cause loosening of the implants [1]. Over the last 30 years, research on bioceramics (ceramics, glass and glass-ceramics) has attracted considerable attention because of their potential for biocompatibility with the human body environment [2]. As hydroxyapatite (HA; $Ca_{10}(PO_4)_6(OH)_2$) contains the main mineral constituents of the natural bones and teeth [1,3], it can bond directly to natural bones. However, the brittle nature and poor strength of HA impedes its clinical applications under load-bearing conditions. Owing to the brittle nature of HA, secondary constituent materials such as carbon nanotubes (CNTs), alumina (Al_2O_3), yttria-stabilized zirconia (YSZ), Ni_3Al and Ti-alloys are often added to enhance its fracture toughness [4–6]. Recently, considerable research has been devoted to the development of HA as a coating material for titanium and/or other metals used in bioimplants [7–14] where the biocompatibility is provided by HA while the mechanical properties of the implant are ensured by the metal substrates [15,16]. Although the US Food & Drug Administration (FDA) has approved plasma spray techniques for coating implants with biocompatible materials, there remains a need to further improve the mechanical properties of HA coating, especially for clinical applications involving load-bearing conditions.

Since their discovery by Iijima [17], carbon nanotubes (CNTs), seamless cylinders of graphite sheets either in the

* Corresponding author. Tel.: +1 305 348 1701; fax: +1 305 348 1932.
E-mail address: agarwala@fiu.edu (A. Agarwal).

1742-7061/$ - see front matter
doi:10.1016/j.actbio.2007.06.001

form of single-walled (SW) or multi-walled assemblies, have been the focus of considerable scientific research due to their outstanding mechanical properties and chemical stability. Several applications have been proposed recently for CNTs, many of which were based on the addition of a small amount of CNTs into a ceramic matrix to produce tougher ceramic materials [18–23]. For example, Zhan et al. [18] fabricated CNT/alumina nanocomposite by blending dispersed single-walled carbon nanotubes with nanocrystalline alumina powders, followed by the spark plasma sintering (SPS) process. The results based on indentation measurements showed threefold improvements in fracture toughness compared with that of an unreinforced nanocrystalline alumina. Therefore, the excellent mechanical properties of CNTs were taken advantage of in the fabrication of the bioceramic nanocomposite in the current work. In a recent work by the authors [24] a 56% enhancement in the fracture toughness of a plasma-sprayed HA-CNT coating was observed. Subsequently human osteoblast hFOB 1.19 cell culture demonstrated biocompatibility of these coatings without deterioration of the cell adhesion, proliferation and differentiation [24]. In addition, CNTs have shown to assist the mineralization of apatite and encourage cell ingrowth [25,26].

It is well understood that wear of the HA coating signals the potential degradation failure of orthopedic implants [27–29] and therefore much effort is needed to investigate the tribological behavior of the artificial biomaterials in the bioenvironment. Also, these implants are seldom used in dry conditions and are often used in lubricated conditions with body fluids. However, very limited information is available in the open literature regarding the wear resistance of HA-CNT composite coating in the physiological environment [30]. Hence, the aim of the present research is to investigate the tribological behavior and overall integrity of plasma-sprayed CNT-reinforced HA composite coating on Ti–6Al–4V in simulated body fluid (SBF) environment.

2. Experimental procedure

The powder feedstock for plasma spraying was prepared by blending irregular HA powder (particle size 10–50 μm) with 4 wt.% multi-walled CNTs (95 + % pure with amorphous C < 2.0%, Ni < 2.0%, Ti < 1.0% and traces (<0.35%) of Cr, Fe, Cu, Si, Zn and Mn) of diameter ranging from 40 to 70 nm and length ranging from 0.5 to 2 μm in a jar mill for 18 h. Plasma spraying of HA with and without CNTs was carried out using a Praxair SG-100 gun with optimized spray parameters. Powders were internally injected in the plasma gun using argon as the carrier gas to coat Ti–6Al–4 V substrate (50 mm × 50 mm × 2 mm). The detailed information on the plasma spraying can be obtained from our previous work [24].

The wear performance of the coated specimens in the SBF environment was evaluated using a pin-on-disc wear tester with an arrangement for the wear testing in an aqueous media. The SBF used in the wear test was prepared according to the procedures discussed in the preparation of conventional c-SBF [30]. The schematic of the wear set-up is illustrated in Fig. 1. A 50 mm long and 3 mm diameter zirconia (ZrO_2) pin was used to slide against the coated specimens. Zirconia is often used as material for the ceramic cup that mates with the metallic stem or ceramic head in total hip replacement surgery. Abrasion of HA coatings by ZrO_2 pin in SBF can illuminate the wear behavior of artificial body implants in human blood plasma to certify overall mechanical integrity.

To ensure the close contact between the pin and the test specimen, the cross-section of the pin was polished using a series of emery papers (240–600 grit size) to form a flat contact surface. Specimens of size 25 mm × 25 mm × 2.2 mm with the HA-CNT coated surface in contact with the flat cross-sectional area of the pin were used. The specimen was clamped and supported on the sample stage located at the bottom of the wear cell filled with SBF. The level of SBF in the wear cell was maintained such that the specimen

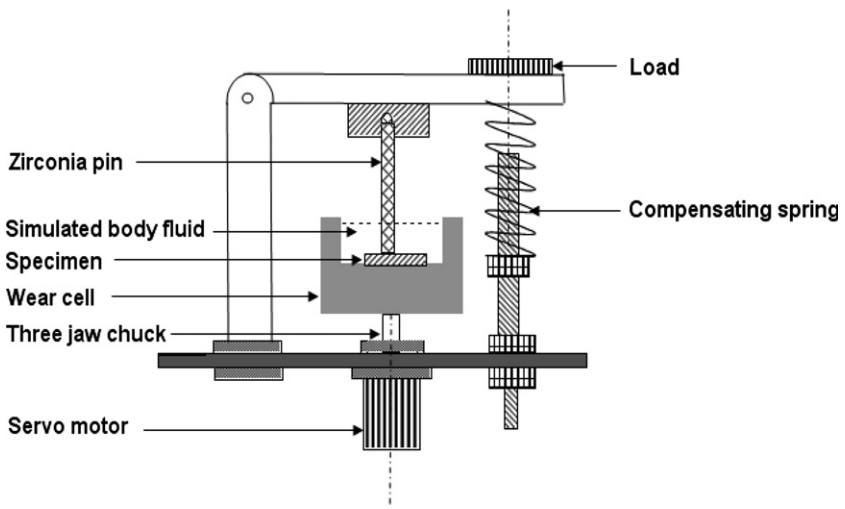

Fig. 1. Schematic illustration of pin-on-disk wear in SBF environment apparatus.

remained immersed in the fluid during the entire duration of the test. A wear test was conducted with a stationary pin and the wear cell rotating at a speed of 100 rpm under a normal load of 8.8 N. The axis of the pin was offset from the axis of specimen rotation by 3 mm such that the inner track radius corresponded to 1.5 mm and the width of the circular wear track corresponded to 3 mm (equal to the diameter of the pin). The total duration of the wear test was 100 min and the weight loss of the specimen was recorded every 10 min using Sartorius digital balance with an accuracy of measurement up to 10^{-4} g. The data were reported in terms of the cumulative weight loss as a function of time and also in terms of wear rate, defined as total weight loss per unit contact area per 10,000 revolutions (corresponding to a linear distance of 188.4 m) for each specimen. Change in the surface topography of the wear tracks was characterized by measuring the roughness using a Mahr M1 perthometer. For each specimen, five roughness measurements were carried out and the average value is reported along with positive and negative error bars. The morphologies of the wear tracks were observed in a field emission scanning electron microscope (JEOL JSM 6330 F).

3. Results

3.1. Background

Plasma spraying of HA-CNT was successfully portrayed in our earlier work [24], demonstrating enhanced crystallinity (by 27%) and fracture toughness (by 56%) when compared with that of plasma-sprayed HA without CNT reinforcement. Uniform deposition of HA-CNT coating (thickness ~120 μm) by plasma spraying is shown in the cross-sectional image (Fig. 2a). Cell growth on HA-CNT surface is observed in Fig. 2b, indicating biocompatibility of this coating. It is important to note that biocompatibility and toxicity of CNTs have been debated in terms of (i) cell growth and proliferation and (ii) free CNTs in the blood/body. Several researchers have demonstrated unrestricted human osteoblast hFOB 1.19 cell growth, adhesion and proliferation, indicating biocompatibility of CNTs

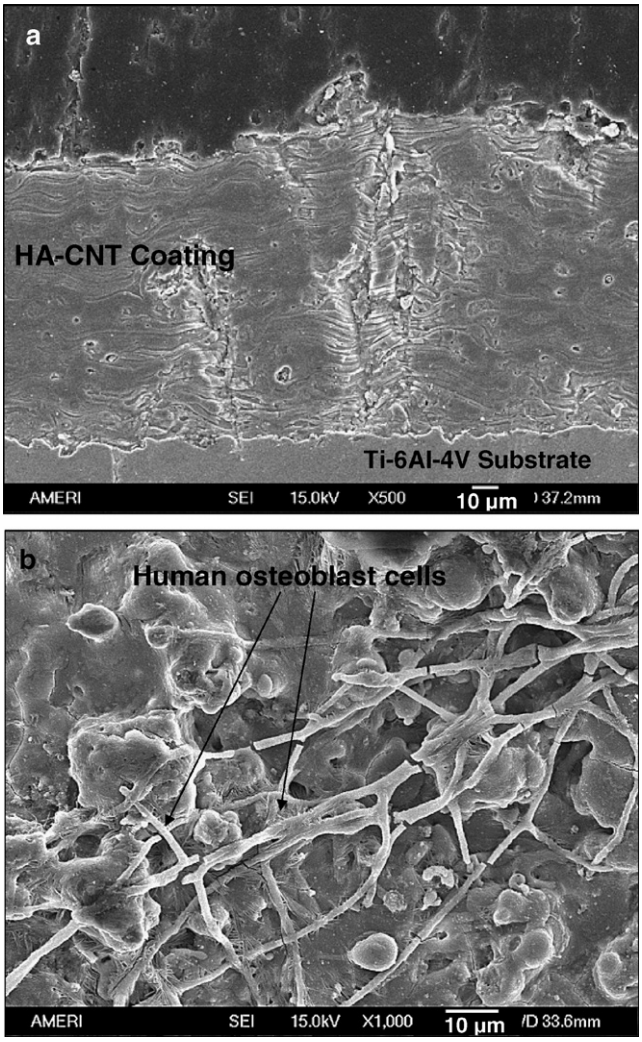

Fig. 2. (a) Cross-sectional image of plasma sprayed HA-CNT coating, and (b) Cell growth, adhesion and proliferation of human osteoblasts on plasma sprayed HA-CNT coating.

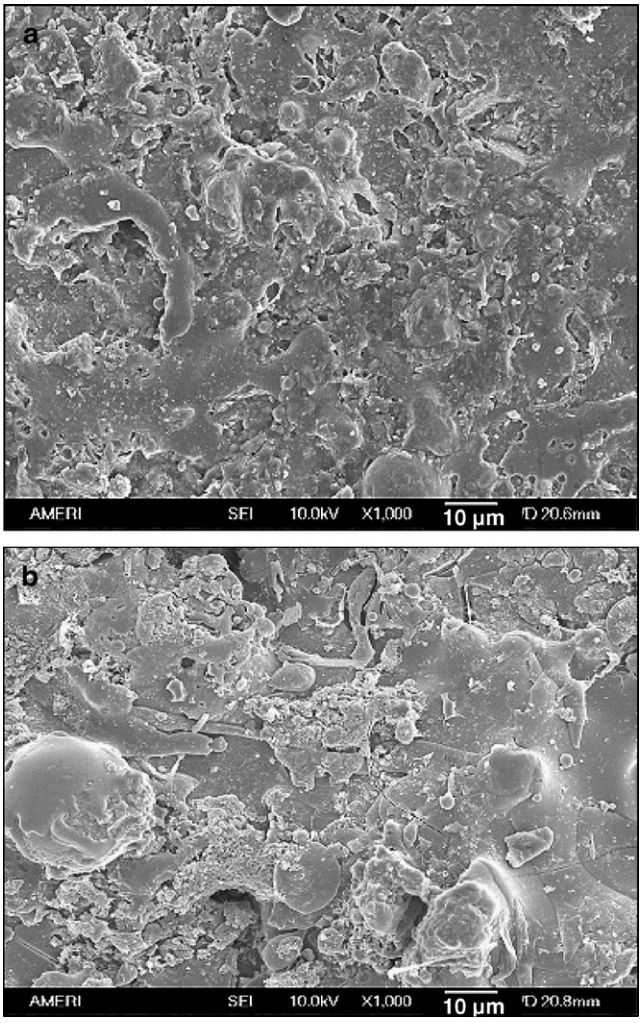

Fig. 3. Top surface of plasma sprayed (a) HA, and (b) HA-CNT coating eliciting surface undulations.

[24,31]. However, the effect of free CNTs in the human body is a relatively unexplored area and there is neither agreement nor consensus on the role of CNTs in vivo [31]. Further sacrificial studies may be required before the CNT-reinforced coatings can be approved by the FDA for implantation in the human body. Since plasma-sprayed HA coatings may degrade with time in vivo, issues of CNT biocompatibility and toxicity cannot be neglected.

Surface roughness (initial and during life), surface interaction with surrounding cells, microstructural assistance for enhanced mechanical properties and consequent wear response in the physiological environment are the key requirements for coated implants in vivo. Pre- and post-wear surface characterization and abrasion response of plasma-sprayed coatings (and bare Ti–6Al–4V substrate) are compared in an SBF environment in the following sections.

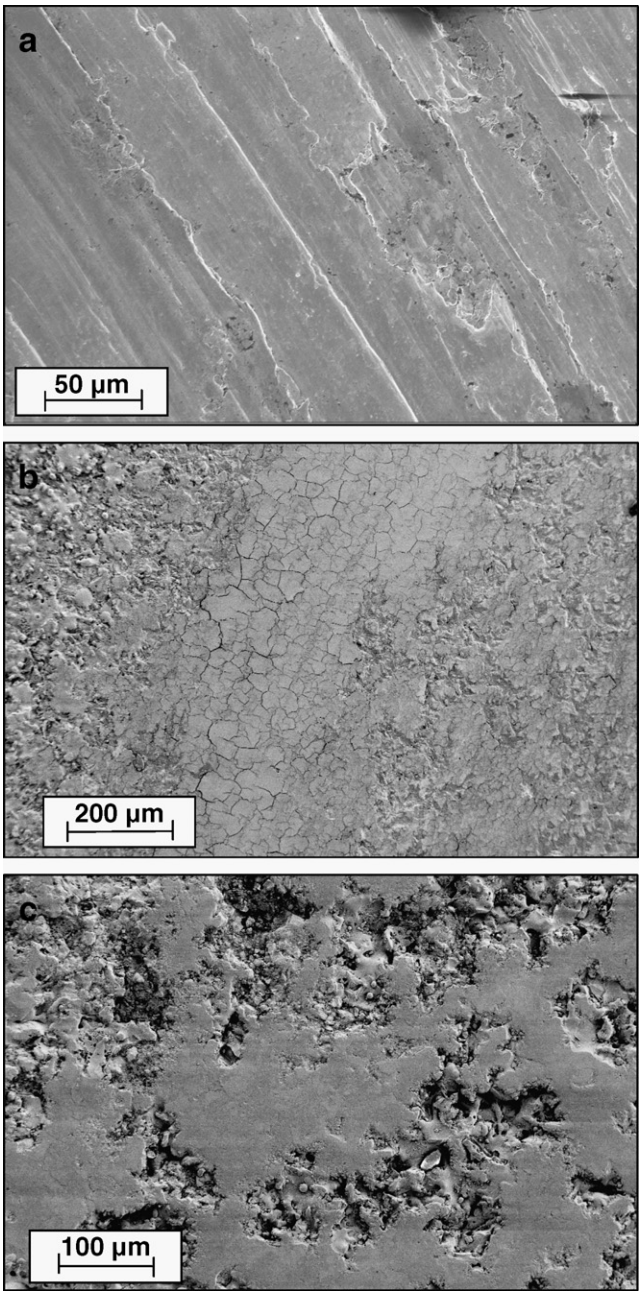

Fig. 4. SEM images of worn surfaces of: (a) Ti–6Al–4V substrate, (b) Plasma sprayed HA coating, and (c) Plasma sprayed HA-CNT coating.

3.2. Surface morphology of plasma-sprayed coatings

Fig. 3 presents the surface topography of the plasma-sprayed HA and HA-CNT coatings on titanium alloy substrate. The figure clearly indicates that HA-CNT coatings have substantial surface undulations compared with HA coatings, which exhibit a smoother surface. The average surface roughness of the HA (Ra ~ 2.496 μm) and HA-CNT (Ra ~ 4.474 μm) coatings was higher than that of Ti–6Al–4V (Ra ~ 0.702 μm), suggesting the development of a complex surface topography under plasma spraying conditions. A scanning electron microscopy overview of the morphology of the wear tracks in Ti–6Al–4V substrate, HA coating and HA-CNT coating is presented in Fig. 4. The physical characterization of these worn surfaces indicates severe wear of Ti–6Al–4V compared with both coatings in SBF. The worn surface of Ti–6Al–4V possesses deep scratches, suggesting poor wear resistance of the base material (Fig. 4a). The worn surface of HA coating has the appearance of a cellular network of interconnected surface cracks, indicating the release of residual stresses through the generation of new surfaces (Fig. 4b), whereas the worn surface of HA-CNT coating has several flat and small islands without any cracks (Fig. 4c). Since the average values of ridges and grooves translate to roughness, the visually smooth appearance of the HA-CNT coating (Fig. 4c) should not be misconstrued as a low Ra value.

It is confirmed by comparison of the roughness of as-sprayed coatings and coatings after the wear test that surface roughness in plasma-sprayed coatings decreases after wear: for HA coating from an Ra of ~2.496 to ~0.868 μm and for HA-CNT coating from an Ra of ~4.474 to ~1.785 μm, whereas the surface roughness of Ti–6Al–4V increased from an Ra of ~0.0702 to ~1.144 μm (Fig. 5). Such a difference in the surface topographies of the coatings

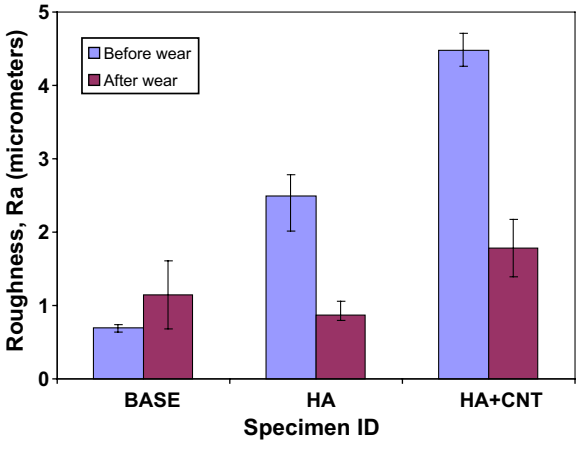

Fig. 5. Bar chart showing the roughness of surfaces before and after wear.

and the substrate is influenced by factors such as the physical/mechanical properties of the coating/substrate system and their response during wear by ZrO_2 pin.

3.3. Wear rate of plasma-sprayed coatings

Superior wear resistance is observed for HA (wear rate ~60.15 g m^{-2} per 10,000 revolutions) and HA-CNT (wear rate ~38.92 g m^{-2} per 10,000 revolutions) coatings when compared with that of bare substrate (wear rate ~90.23 g m^{-2} per 10,000 revolutions). Fig. 6a shows that the wear resistance of the CNT-reinforced HA composite coating is the highest. Cumulative weight loss of the Ti–6Al–4V and plasma-sprayed HA and HA-CNT coatings is shown in Fig. 6b. The temporal weight loss response indicates the high sliding wear resistance of HA-CNT coating (total weight loss ~0.0022 g), followed by HA coating (total weight loss ~0.0034 g) and Ti–6Al–4V substrate (total weight loss ~0.0051 g) after 100 min of wear test. Wear in terms of volume loss was also computed by multiplying the mass loss by the material density. The porosity in the HA-based coatings was obtained using quantitative microscopy and image analysis. The porosity of the HA coating was 4.9% (95.1% of theoretical density of HA), whereas that of the HA-CNT coating was 6.2% (93.8% dense of theoretical density of HA + 4wt.% CNT). Wear in terms of volume loss of 0.001154, 0.00134 and 0.000754 cc was obtained for Ti–6Al–4V, HA coating and HA-CNT coating, respectively. The results show the lowest volume loss for HA-CNT coating, indicating its highest wear resistance.

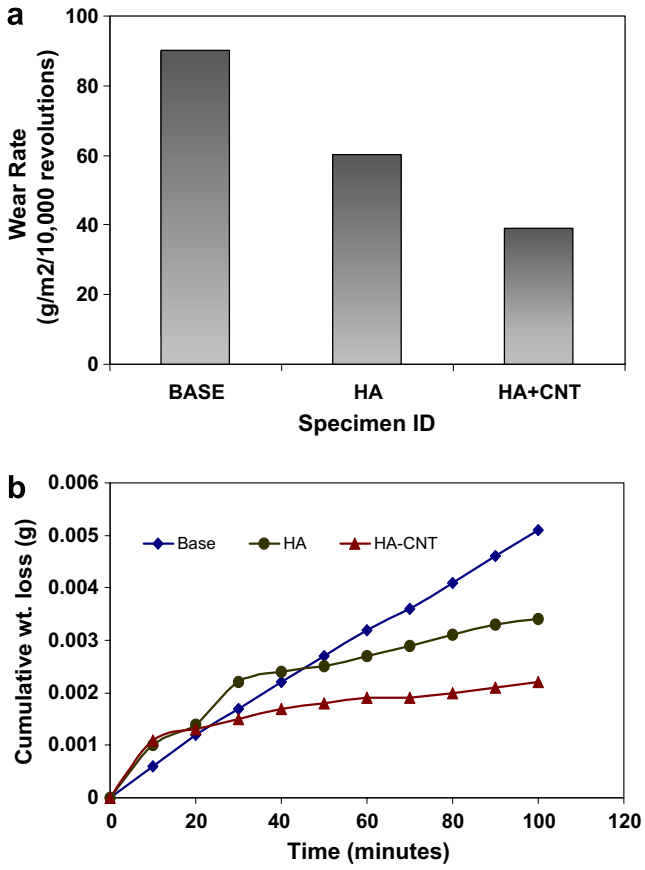

Fig. 6. (a) Comparative bar chart showing wear rate of uncoated (base) and coated (plasma sprayed HA and HA-CNT) samples, and (b) Weight loss of various materials with wear-time.

4. Discussion

4.1. Effect of surface roughness on wear

Post-wear surface roughness and topography is an indicator of underlying wear mechanism. Primary weight loss of metallic Ti–6Al–4V implant substrate is caused by adhesive wear. Ti–6Al–4V is softer than the counter-contact zirconia pin. Hence, the zirconia pin penetrates into the metallic substrate, generating successive scratch marks. Because of the continuous adhesive wear of the Ti–6Al–4V substrate, the surface roughness increased from an Ra of ~0.0702 to ~1.144 μm. Extensive damage to the Ti–6Al–4V substrate is attributed to the plastic deformation followed by shearing and consequent material removal upon scratching by the zirconia pin.

Wear in plasma-sprayed ceramic coatings is caused by different mechanisms, such as abrasion, fracture, plastic deformation fragmentation, chipping and ploughing. Pre-worn surface roughness influences the abrasion wear response of coated specimens. The high surface roughness of plasma-sprayed HA and HA-CNT coatings is expected to provide a relatively small contact area for loading (due to the greater roughness) and, when combined with the

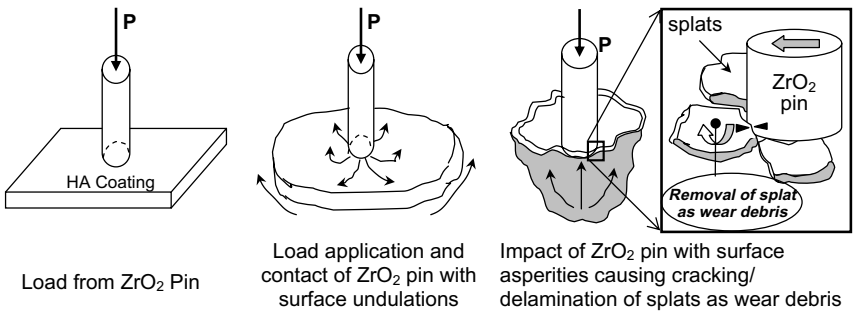

Fig. 7. Schematic of chipping of splats as wear debris through ZrO_2 pin abrasion.

counter motion of ZrO_2-pin against HA coating, it induces impact, resulting in surface-chipping through cracking/delamination of splats, as shown schematically in Fig. 7. Successive ZrO_2 abrasion with the cracked/delaminated surface peels off the individual splats. This explains the development of the cellular network of interconnected cracks in the plasma-sprayed HA coating (Fig. 4b) that consequently separates it out as wear debris.

Higher weight loss of both plasma-sprayed HA coatings in the initial (~20 min) wear stage is attributed to their higher initial roughness (HA: Ra ~ 2.496 μm and HA-CNT: Ra ~ 4.474 μm) compared with Ti–6Al–4V (Ra ~ 0.702 μm) (Fig. 5). Since a higher surface roughness brings surface protrusions (asperities) in direct contact with the ZrO_2 abrading pin, the direct impact causes severe splat chipping. These asperities fracture and separate from the substrate when the sliding forces exceed the fracture strength of the material. Therefore, during the initial part of the wear cycle, weight loss is higher; it eventually drops down to reach a constant value (Fig. 6b). The subsequent substantial reduction in the weight-loss and equilibrium wear-plateau in HA-CNT coating are attributed to CNT's antifriction properties and anchoring of delaminated splats via CNT stretching, as explained in the following section.

4.2. Effect of CNT reinforcement on wear

The reduced wear rate of the plasma-sprayed HA-CNT coating is attributed to CNT reinforcements which act as bridges to connect splats (Fig. 8a and b) and restrict the separation of adjacent splats. Fig. 8a shows the anchoring of splats by CNT, which provides added reinforcement by locking the splats in place. Furthermore, release of wear debris is reduced by the pinning of HA islands by stretched CNTs (Fig. 8c). Both phenomena indicate that wear debris is secured by CNT anchors, allowing limited damage to the HA-CNT coating via chipping. Retention of delaminated splats confirms the greater roughness of the post-wear HA-CNT coating (Fig. 5) compared with that of the HA coating without CNT. This also ensures that wearing of the surface occurs only by the smoothing out of surface asperities by the zirconia pin and not by wear-debris damage. As observed from the fracture toughness improvements of up to 56% in the CNT-reinforced HA coatings [24], the presence of CNTs affirm pinning and fastening of HA by the formation of hooks and bridges.

It has been indicated by researchers that CNTs provide lubricating conditions during the severe abrasion [32] between the ZrO_2 pin and the coatings, thereby reducing the wear of ceramic coatings. CNT underprops become significant lubricating regions that retain cohesion with the matrix and reduce weight loss by protecting the abrading surface. It is interesting to note that CNTs distribute over the worn surface to form a horn-like structure under the effect of repeated grinding of the counterpart (Fig. 9a). Embedded CNTs appeared to have strong cohesion with the matrix elements, whereas surface dangling CNTs act as energy-absorbing sources during abrasion. Thus, fracture toughness is synergistically increased via limited

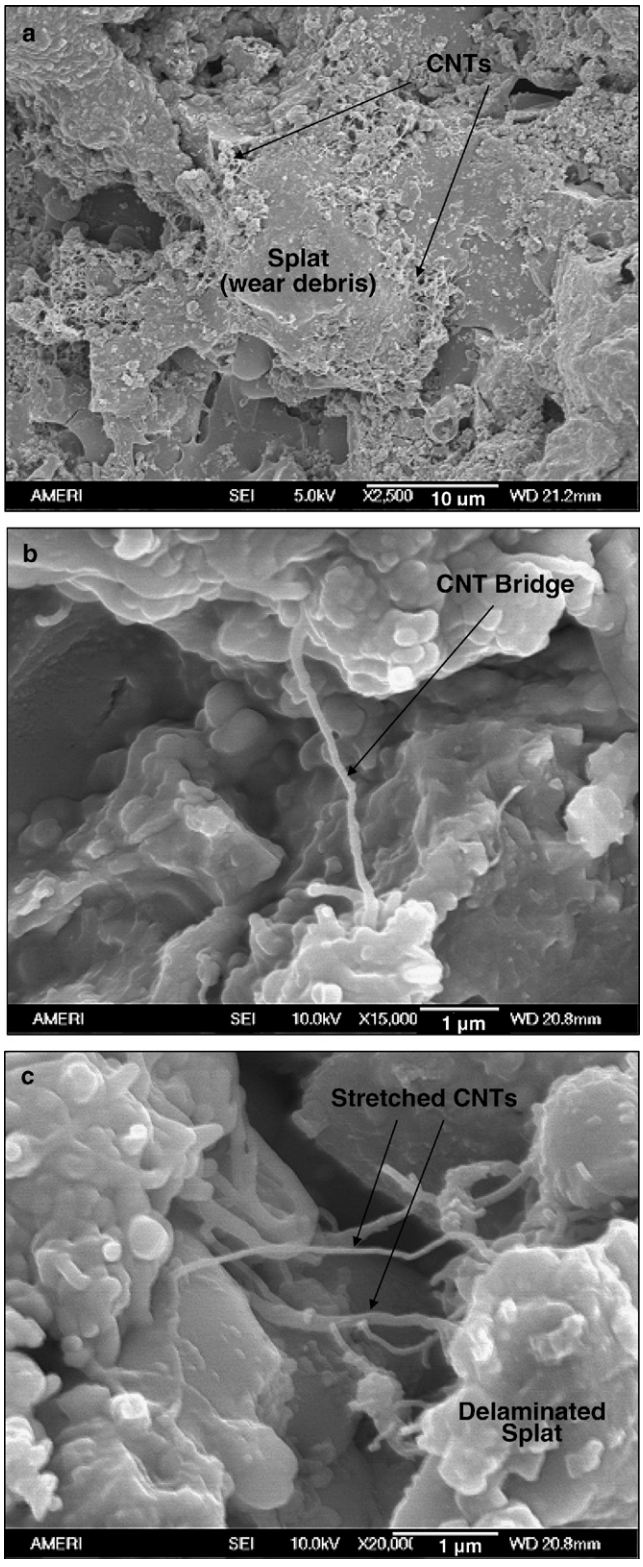

Fig. 8. (a) Wear surface of plasma sprayed HA-CNT coating depicting splat anchoring by CNTs and high magnification SEM views showing (b) CNT bridging of splats, and (c) Anchoring of wear debris by stretched CNTs.

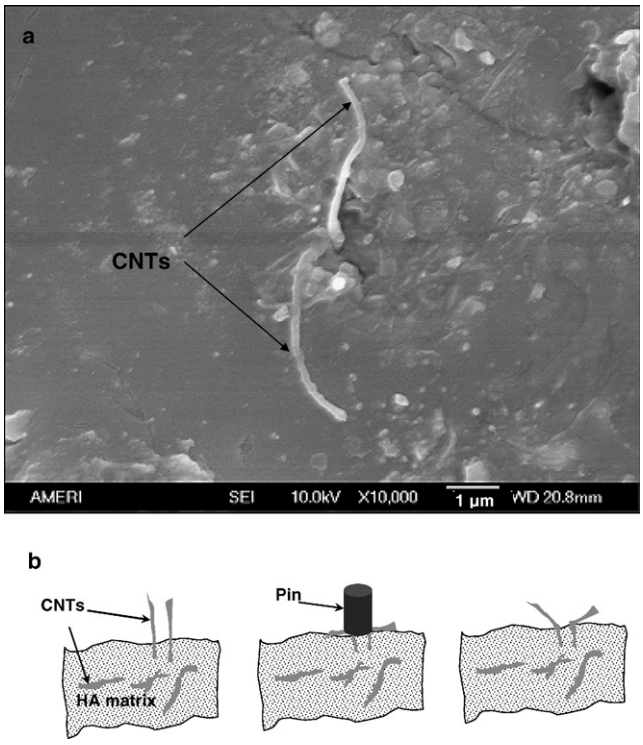

Fig. 9. (a) Horn-like structure formed by the dangling CNTs on the worn surface of plasma sprayed HA-CNT coating, and (b) Schematic illustration of the formation of CNT horn on the worn surface.

damage of the coating due to the combined effect of anchoring by CNTs within the matrix of coating and energy absorbing at the surface of the coating by horn-like CNT structures. The schematic of the formation mechanism of the CNT horn is illustrated in Fig. 9b. CNTs protrude from the top surface of the composite coating either during spraying or due to the removal of surrounding material during wear. These CNTs bend when the pin repeatedly passes over them, leading to the formation of horn-like CNT through partial elastic recovery after the wear cycle (Fig. 9b). As observed in Fig. 9a, the increased thicknesses (increase in the original diameter from 40–70 nm to greater than 200 nm) of CNTs imply that the CNTs become coated with HA during the plasma spraying. The lubricating nature of tubular CNTs, assisted by surface protection with sn HA melt coating, results in a composite morphology that is ideal for sustained enhanced abrasion resistance. Therefore, a CNT-reinforced HA composite coating would be expected to provide improved mechanical properties and biocompatibility, and hence be a potential synthetic replacement implant material under high load-bearing conditions.

5. Conclusions

Wear studies were performed on plasma-sprayed HA and HA-CNT coatings under SBF conditions to determine the material response in vitro. Both HA and HA-CNT coatings demonstrated superior wear resistance when compared with body implant Ti–6Al–4V substrate. HA-CNT coatings result in reduced weight and volume loss during wear (in comparison to HA coatings and Ti–6Al–4V substrate). Apart from the underpropping and self-lubricating nature of CNTs, CNT bridging and stretching assist the pinning of wear debris, consequently resulting in reduced weight and volume loss of plasma-sprayed HA-CNT coating.

Acknowledgements

The authors acknowledge Dr. Tapas Laha and Ms. Melanie Andara in assisting the plasma spraying of samples. Drs. R. Anderson and E. Crumpler in the Biomedical Engineering Department at FIU are acknowledged for assisting with cell-growth studies. K.B. acknowledges an FIU Dissertation Year Fellowship. A.A. acknowledges partial support from ONR grant N00014-05-1-0398 and the FIU Foundation.

References

[1] Suchanek W, Yoshimura M. Processing and properties of hydroxyapatite-based biomaterials for use as hard tissue replacement implants. J Mater Res 1998;13:94–117.
[2] Wang M. Developing bioactive composite materials for tissue replacement. Biomaterials 2003;24:2133–51.
[3] Tadic D, Peters F, Epple M. Continuous synthesis of amorphous carbonated apatite. Biomaterials 2002;23:2553–9.
[4] Hu H, Ni Y, Montana V, Haddon RC, Parpura V. Chemically functionalized carbon nanotubes as substrate for neuronal growth. Nanoletters 2004;4:507–11.
[5] Fang L, Leng Y, Gao P. Processing and mechanical properties of HA/UHMWPE nanocomposites. Biomaterials 2006;27:3701–7.
[6] Peterlik H, Roschger P, Klaushofer K, Fratzl P. From brittle to ductile fracture of bone. Nat Mater 2006;5:52–5.
[7] . Cheng HM. Synthesis, microstructure, properties and applications of carbon nanotubes. In editors. Beijing: Chemistry Press. 2002. p 6.
[8] Ducheyne P, Beight J, Cuckler J, Evans B, Radin S. Effect of calcium phosphate coating characteristics on early post-operative bone tissue ingrowth. Biomaterials 1990;11:531–40.
[9] Weng J, Liu X, Zhang X, Ma Z, Ji X, Zyman Z. Further studies on the plasma-sprayed amorphous phase in hydroxyapatite coatings and its deamorphization. Biomaterials 1993;14:578–82.
[10] Dalton JE, Cook SD, Thomas KA, Kay JF. The effect of operative fit and hydroxyapatite coating on the mechanical and biological response to porous implants. J Bone Joint Surg 1995;77A:97–110.
[11] Klein CPAT, Patka P, Lubbe HBMVd, Wolke JGC, Grook KD. Plasma-sprayed coating of tetracalcium phosphate, hydroxyapatite, and alpha-TCP on titanium alloy: an interface study. J Biomed Mater Res 1991;25:53–65.
[12] Lynn AK, DuQuesnay DL. Hydroxyapatite-coated Ti–6Al–4V Part 1: The effect of coating thickness on mechanical fatigue behavior. Biomaterials 2002;23:1937–46.
[13] Cheang P, Khor KA, Teoh LL, Tam SC. Pulsed laser treatment of plasma-sprayed hydroxyapatite coatings. Biomaterials 1996;17:1901–4.
[14] Kurella A, Dahotre NB. Laser induced hierarchical calcium phosphate structures. Acta Biomater 2006;2:677–83.
[15] Singh R, Kurella A, Dahotre NB. Laser surface modification of Ti–6Al–4V: wear and corrosion characterization in simulated biofluids. J Biomater Appl 2006;21:46–72.
[16] Singh R, Dahotre NB. Tribology of laser modified surface of stainless steel in physiological solution. J Mater Sci 2005;40:5619–26.

[17] Iijima S. Helical microtubules of graphitic carbon. Nature 1991;354:56–8.
[18] Zhang GD, Kuntz JD, Wan JL, Mukjherjee AK. Single-wall carbon nanotubes as attractive toughening agents in alumina-based nanocomposites. Nat Mater 2003;2:38–42.
[19] Baughman RH, Zakhidov AA, Heer WAd. Carbon nanotubes–the route towards applications. Science 2002;297:787–92.
[20] Thostenson ET, Ren ZF, Chou TW. Advances in the science and technology of carbon nanotubes and their composites: a review. Comp Sci Technol 2001;61:1899–912.
[21] Dai HJ. Carbon nanotubes: opportunities and challanges. Surf Sci 2002;500:218–43.
[22] Lupo F, Kamalakaran R, Scheu C, Grobert N, Ruhle M. Microstructural investigations on zirconium oxide–carbon nanotube composites synthesized by hydrothermal crystallization. Carbon 2004;42:1995–9.
[23] Chen Y, Gan CH, Zhang TN, Yu G, Bai PC, Kaplon A. Laser-surface-alloyed carbon nanotubes reinforced hydroxyapatite composite coating. Appl Phys Lett 2005;85:251905.
[24] Balani K, Anderson R, Laha T, Andara M, Tercero J, Crumpler E, Agarwal A. Plasma-sprayed carbon-nanotube reinforced hydroxyapatite coatings and their interaction with human osteoblasts in vitro. Biomaterials 2006; doi:10.1016/j.biomaterials.2006.1009.1013.
[25] Zhao B, Hu H, Mandal SW, Haddon RC. A Bone mimic based on the self-assembly of hydroxyapatite on chemically functionalized single-walled carbon nanotubes. Chem Mater 2005;17:3235–41.
[26] Akasaka T, Watari F, Sato Y, Tohji K. Apatite formation on carbon nanotubes. Mater Sci Eng C 2006;26:675–8.
[27] Coathup MJ, Blackburn J, Goodship AE, Cunnigham JL, SMith T, Blunn GW. Role of hydroxyapatite coating in resisting wear particle migration and osteolysis around acetabular components. Biomaterials 2005;26:4161–9.
[28] Morks MF, Kobayashi A, Fahim NF. Abrasive wear behavior of sprayed hydroxyapitite coatings by gas tunnel type plasma spraying. Wear 2006; doi:10.1016/j.wear.2006.1005.1013.
[29] Hukovic MM, Tkalcec E, Kwokal A, Piljac J. An in vitro study of Ti and Ti-alloys coated with sol–gel derived hydroxyapatite coatings. Surf Coat Technol 2003;165:40–50.
[30] Oyane A, Kim HM, Furuya T, Kokubo T, Miyazaki T, Nakamura T. Preparation and assessment of revised simulated body fluids. Biomed Mater Res A 2003;65:188–95.
[31] Smart SK, Cassady A, Lu GQ, Martin DJ. The biocompatibility of carbon nanotubes. Carbon 2006;44:1034–47.
[32] Li ZH, Wang XQ, Wang M, Wang FF, Ge HL. Preparation and tribological properties of the carbon nanotubes –Ni–P composite coating. Tribol Int 2006;39:953–7.